

## Spectroscopic Studies on the Higher Binary Fluorides of Chromium : CrF<sub>4</sub>, CrF<sub>5</sub>, and CrF<sub>6</sub>, both in the Solid State and Isolated in Inert Gas Matrices †

Eric G. Hope, Peter J. Jones, William Levason,\* J. Steven Ogden,\* Mahmoud Tajik, and Jeremy W. Turff

Department of Chemistry, The University, Southampton SO9 5NH

Pure samples of CrF<sub>4</sub>, CrF<sub>5</sub>, and CrF<sub>6</sub>, together with the related salts CsCrF<sub>6</sub> and Cs<sub>2</sub>CrF<sub>6</sub>, have been prepared, and a number of spectroscopic measurements made. In particular, the solid state i.r. and u.v.–visible spectra of CrF<sub>4</sub> and CrF<sub>5</sub> indicate fluorine-bridged polymeric structures, whilst CsCrF<sub>6</sub> and Cs<sub>2</sub>CrF<sub>6</sub> contain essentially discrete CrF<sub>6</sub> units. Matrix isolation studies on CrF<sub>4</sub> and CrF<sub>5</sub> lead to the identification of molecular CrF<sub>4</sub> (*T<sub>d</sub>*) and CrF<sub>5</sub> (*O<sub>h</sub>*) which are characterised by intense i.r. bands at 784.3 and 763.2 cm<sup>-1</sup> respectively (argon matrices); the vapourisation of CrF<sub>5</sub> is shown to yield CrF<sub>4</sub> + CrF<sub>6</sub> by disproportionation. The u.v.–visible spectrum of CrF<sub>6</sub> contains prominent charge-transfer bands at *ca.* 38 450 and *ca.* 26 700 cm<sup>-1</sup>.

Five binary fluorides of chromium have been reported,<sup>1</sup> namely CrF<sub>2</sub>, CrF<sub>3</sub>, CrF<sub>4</sub>, CrF<sub>5</sub>, and CrF<sub>6</sub>, of which only the first two have been studied in detail. The three higher fluorides are very difficult to obtain in even a reasonably pure state, and their corrosive nature has in general hampered investigations,<sup>2-9</sup> although some spectroscopic data have been reported.<sup>10-13</sup> However, for CrF<sub>6</sub>, the extreme conditions of the literature synthesis<sup>3</sup> and its reported thermal instability (decomposing  $\geq$  *ca.* 150 K), have essentially precluded all studies.

As an extension of our earlier work on the synthesis and characterisation of chromium oxohalides (CrOCl<sub>3</sub>,<sup>14</sup> CrOF<sub>3</sub>,<sup>15</sup> CrOF<sub>4</sub>,<sup>16</sup> and CrO<sub>2</sub>F<sub>2</sub><sup>17</sup>) we have recently completed detailed i.r. and u.v.–visible studies on CrF<sub>4</sub>, CrF<sub>5</sub>, and CrF<sub>6</sub> both in the solid state and also using matrix isolation techniques. A preliminary account of our work on CrF<sub>6</sub> has been the subject of a recent communication;<sup>18</sup> this present paper discusses in detail the synthesis and spectroscopic results obtained for all three higher binary fluorides, and for the related salts CsCrF<sub>6</sub> and Cs<sub>2</sub>CrF<sub>6</sub>.

### Experimental

The preparation of the higher chromium fluorides has generally involved the fluorination of either chromium powder, CrF<sub>3</sub>, or CrO<sub>3</sub> using both flow and static methods. We have explored both these methods, and attempted a large number of syntheses under a wide variety of conditions. Relatively few of these yielded pure materials, ‡ as the conditions necessary for preparation proved to be rather critical. Elemental analyses were performed using standard reagents as described previously.<sup>15</sup>

**Synthesis of CrF<sub>4</sub>.**—Chromium tetrafluoride was made by static fluorination of CrF<sub>3</sub>, and also by a flow method from chromium powder and fluorine similar to that described by Clark and Sadana.<sup>9</sup> This latter route proved to be more satisfactory, and in a typical preparation, powdered electrolytic grade chromium (4 mmol) was placed in a nickel boat inside a copper tube and heated to 350 °C for 30 min in a stream of fluorine. After cooling in a stream of argon, the apparatus was transferred to a dry-box, and dark green CrF<sub>4</sub> removed (Found: Cr, 47.7; F, 52.1. Calc. for CrF<sub>4</sub>: Cr, 47.7; F, 52.3%).

**Synthesis of CrF<sub>5</sub>.**—Samples of dark red CrF<sub>5</sub> were most conveniently prepared by static fluorination of CrF<sub>3</sub> using a procedure similar to that described by Slivnik and Zemva.<sup>7</sup> In a typical preparation, CrF<sub>3</sub> (Cerac) (15 mmol) was loaded into a Monel autoclave (300 cm<sup>3</sup>) in a dry-box, and after evacuation, F<sub>2</sub> was admitted to a pressure of 30 atm. After heating at 350 °C for 2 h, the autoclave was cooled to room temperature. The excess F<sub>2</sub> was pumped out, and the autoclave evacuated to 10<sup>-1</sup> Torr for several hours. The autoclave was subsequently opened in a dry-box and sticky red CrF<sub>5</sub> was removed from the lid (Found: Cr, 35.3; F, 64.6. Calc. for CrF<sub>5</sub>: Cr, 35.4; F, 64.6%).

**Synthesis of CrF<sub>6</sub>.**—The original preparation of CrF<sub>6</sub> described by Glemser *et al.*<sup>3</sup> involved the static fluorination of chromium powder under extreme conditions (350 atm F<sub>2</sub>, 400 °C). Our samples of CrF<sub>6</sub> were obtained under somewhat milder conditions by the static fluorination of CrO<sub>3</sub> in a pre-fluorinated Monel autoclave fitted with a water-cooled lid.

The course of this reaction proved to be very dependent upon temperature and pressure. Under moderate F<sub>2</sub> pressures (*ca.* 4 atm) the principal product at 120 °C (24 h) was found to be CrO<sub>2</sub>F<sub>2</sub>, whilst at *ca.* 140 °C (72 h) a mixture of CrO<sub>2</sub>F<sub>2</sub> and CrOF<sub>4</sub> was obtained. At *ca.* 200 °C (72 h), increasing amounts of CrF<sub>5</sub> appeared and this is consistent with a mechanism involving the stepwise substitution of oxygen by fluorine to give CrF<sub>6</sub>, followed by thermal decomposition to CrF<sub>5</sub>. It therefore seemed likely that at lower temperatures and higher fluorine pressures this reaction might yield CrF<sub>6</sub>.

In a typical preparation of CrF<sub>6</sub>, the Monel autoclave (300 cm<sup>3</sup>) was loaded in a dry-box with powdered CrO<sub>3</sub> (25 mmol) and, after evacuation, was filled with F<sub>2</sub> to *ca.* 25 atm. The autoclave was then heated to 170 °C for 72 h and allowed to cool, first to room temperature, and subsequently to -63 °C, where it was evacuated to remove the more volatile contents. After warming to room temperature, the autoclave was opened in a dry-box and found to contain deep red CrF<sub>5</sub> on the water-cooled lid, and volatile, lemon-yellow<sup>3</sup> CrF<sub>6</sub> on the walls. This latter product decomposed only slowly (a few days) to CrF<sub>5</sub> when stored in the autoclave, but samples transferred to pre-fluorinated steel containers decomposed within a few hours. Both glass and silica were rapidly attacked by CrF<sub>6</sub> at room temperature, and its hydrolysis reactions were spectacular. In particular, it reacted instantly in air producing an orange smoke, and violently in water to give a greenish yellow solution.

This reactivity and thermal instability precluded a complete analysis, but after hydrolysis the resulting solution gave an

† *Non-S.I. units employed:* atm = 101 325 Pa, Torr = 133 Pa, dyn = 10<sup>-5</sup> N.

‡ Purity was estimated by a combination of elemental analysis and spectroscopic studies: analysis alone is an imperfect guide in this area.<sup>19</sup>

elemental ratio Cr:F of typically 1:5.7, thus confirming that the yellow material was  $\text{CrF}_6$ .

The success of this preparation under much less extreme conditions than those previously reported<sup>3</sup> is almost certainly due to the ease with which the volatile intermediate oxofluorides can exchange oxygen for fluorine. In the direct fluorination of elemental chromium, it is probable that the lower (solid) fluorides are somewhat inert and that much higher temperatures are required for the reaction to proceed to completion. As a result, much higher  $\text{F}_2$  pressures will be needed to prevent decomposition to  $\text{CrF}_5$ .

**Matrix Isolation Studies.**—The general features of our matrix isolation apparatus have been described elsewhere.<sup>20</sup> In these present studies, samples of  $\text{CrF}_4$ ,  $\text{CrF}_5$ , and  $\text{CsCrF}_6$  were vaporised from stainless-steel or Monel tubes at relatively low temperatures, and the vapours co-condensed with an excess of nitrogen or argon matrix gas (B.O.C. 99.999%) onto an optically transparent window cooled to ca. 12 K.

Samples of matrix-isolated  $\text{CrF}_6$  were obtained by simultaneous deposition of a  $\text{CrF}_6$ -matrix gas mixture and a flow of pure matrix gas. In a typical experiment, the autoclave containing a sample of freshly prepared  $\text{CrF}_6$  was cooled to ca.  $-10^\circ\text{C}$  and rapidly pumped out to remove residual volatile impurities. Nitrogen or argon gas was then admitted to atmospheric pressure, and the autoclave connected to the matrix equipment *via* a stainless-steel spray-on line.

There are no reliable vapour pressure data for  $\text{CrF}_6$ , but we estimate that this procedure resulted in a room-temperature  $\text{CrF}_6$ -matrix gas mixture of ca. 1:10. This sample was subsequently co-condensed with an excess of pure inert matrix gas to ensure good isolation. During deposition, the autoclave was at room temperature, but the stainless-steel spray-on line between the autoclave valve and the cryostat could be heated or cooled to investigate the possible thermal decomposition of  $\text{CrF}_6$ .

I.r. spectra were recorded using CsI optics in conjunction with Perkin-Elmer instruments, models 225 and 983G, whilst u.v.-visible spectra were obtained from a Perkin-Elmer 554 instrument, using LiF optics.

## Results and Discussion

**Solid State Studies.**—*Chromium tetrafluoride.* This compound is reportedly amorphous,<sup>2,9</sup> but by analogy with some other transition-metal tetrahalides,<sup>21</sup> it seems probable that its structure is based on edge-sharing  $\text{CrF}_6$  octahedra. This would result in an i.r. spectrum characterised by both terminal and bridging Cr-F stretching modes, and a u.v.-visible spectrum which should show similarities to a  $d^2$  ion in an  $O_h$  environment.

The i.r. spectrum of solid  $\text{CrF}_4$  (Nujol mull) shows strong absorptions in the regions  $830\text{--}750\text{ cm}^{-1}$  ( $\nu_{\text{Cr-F}}$  terminal) and  $550\text{--}490\text{ cm}^{-1}$  ( $\nu_{\text{Cr-F}}$  bridge) and also at ca.  $290\text{ cm}^{-1}$  ( $\delta_{\text{Cr-F}}$ ). The diffuse reflectance spectrum of the solid contains a very broad, intense absorption at  $35\,000\text{--}40\,000\text{ cm}^{-1}$ , strong bands at  $21\,000$  and  $28\,000\text{ cm}^{-1}$ , and weak features at  $12\,350$  and  $13\,500\text{ cm}^{-1}$ . Using the conventional ligand-field approach for a  $d^2$  ion in  $O_h$  symmetry,<sup>22</sup> we assign the most intense features of this spectrum as follows:  $21\,000\text{ cm}^{-1}$  [ ${}^3T_{1g}(F) \rightarrow {}^3T_{2g}$ ],  $28\,000\text{ cm}^{-1}$  [ ${}^3T_{1g}(F) \rightarrow {}^3T_{1g}(P)$ ],  $35\,000\text{--}40\,000\text{ cm}^{-1}$  (F→Cr charge transfer). This assignment yields values:  $Dq = 2\,200 \pm 100\text{ cm}^{-1}$ ,  $B' = 550 \pm 100\text{ cm}^{-1}$ , and taking  $B(\text{Cr}^{4+})$ <sup>22</sup> as  $1\,039\text{ cm}^{-1}$ , a value for  $\beta$  of 0.52. The third spin-allowed band [ ${}^3T_{1g}(F) \rightarrow {}^3A_{2g}$ ] is predicted to lie at ca.  $44\,000\text{ cm}^{-1}$ . Although the actual symmetry will be lower than  $O_h$ , there was no evidence of band splitting. The ligand-field parameters obtained from this analysis compare favourably with those found in the related ion  $[\text{MnF}_6]^{2-}$ , for which  $Dq = 2\,175\text{ cm}^{-1}$  and

$\beta = 0.56$ .<sup>22</sup> The remaining very weak features at  $12\,350$  and  $13\,500\text{ cm}^{-1}$  are assigned as spin-forbidden transitions to singlet states.

*Chromium pentafluoride.* Pure  $\text{CrF}_5$  is hydrolysed rapidly in air, and violently in water to give a solution containing  $\text{Cr}^{\text{III}}$  and  $\text{Cr}^{\text{VI}}$  species. It inflames ammonia and most organic materials on contact, and is a very strong fluorinating agent.<sup>8</sup> I.r. and Raman studies on the liquid<sup>11</sup> indicate a fluorine-bridged octahedral structure, and in particular, i.r. bands have been reported at  $820\text{--}650$ ,  $580\text{--}400$ , and ca.  $250\text{ cm}^{-1}$ . Preliminary X-ray data are available for the solid,<sup>4</sup> but there are no published u.v.-visible or i.r. studies in this phase.

We have obtained an i.r. spectrum of solid  $\text{CrF}_5$ , pressed between plastic discs, which shows broad intense absorptions at  $830\text{--}750$ ,  $600\text{--}450$ , and ca.  $300\text{ cm}^{-1}$ , and assign these as  $\nu_{\text{Cr-F}}$  (terminal),  $\nu_{\text{Cr-F}}$  (bridge), and  $\delta_{\text{FCrF}}$  modes respectively. The diffuse reflectance u.v.-visible spectrum contained bands at  $22\,400$ ,  $26\,000$ , and  $37\,000\text{ cm}^{-1}$ , and these are interpreted in terms of a  $d^1$  species in a low-symmetry environment. In particular, we assign the two lowest bands to the (split)  ${}^2T_{2g} \rightarrow {}^2E_g$  transition in  $O_h$  symmetry and this leads to a value of ca.  $2\,400\text{ cm}^{-1}$  for the parameter  $Dq$ . The broad absorption at  $37\,000\text{ cm}^{-1}$  is then assigned as the lowest F→Cr charge transfer (c.t.) band. These assignments result in reasonable agreement with the  $Dq$  value for  $\text{CrF}_4$  ( $2\,200\text{ cm}^{-1}$ , see above) and with a prediction of  $36\,000 \pm 2\,000\text{ cm}^{-1}$  for the position of the c.t. band based on the optical electronegativity model.<sup>23</sup>

$\text{CsCrF}_6$  and  $\text{Cs}_2\text{CrF}_6$ . Spectroscopic data on  $\text{Cr}^{\text{V}}$  and  $\text{Cr}^{\text{IV}}$  compounds are very limited, and we therefore prepared small amounts of these materials, using literature methods,<sup>8,24</sup> for comparative purposes. Both were found to show a single, very broad, intense absorption in the i.r. spectrum at ca.  $600$  ( $\text{CsCrF}_6$ ) and ca.  $580\text{ cm}^{-1}$  ( $\text{Cs}_2\text{CrF}_6$ ), in good agreement with the literature,<sup>8,24</sup> and these features are assigned to terminal Cr-F stretching modes in the essentially discrete anions  $[\text{CrF}_6]^-$  and  $[\text{CrF}_6]^{2-}$ . The diffuse reflectance spectrum of  $\text{CsCrF}_6$  shows bands at ca.  $21\,100$  (sh),  $24\,150$ , and  $30\,000\text{--}43\,000\text{ cm}^{-1}$ . The two lower energy features are assigned as the  ${}^2B_{2g} \rightarrow {}^2A_{1g}$  and  ${}^2B_{2g} \rightarrow {}^2B_{1g}$  transitions in the Jahn-Teller distorted anion ( $D_{4h}$ ), whilst the higher energy absorption is F→Cr c.t. These features are thus very similar to those observed for  $\text{CrF}_5$ .

Our samples of  $\text{Cs}_2\text{CrF}_6$  showed a diffuse reflectance spectrum similar to that published for  $\text{Rb}_2\text{CrF}_6$ .<sup>24</sup> An intense F→Cr c.t. band was observed in the region  $30\,000\text{--}40\,000\text{ cm}^{-1}$ , and weaker  $d-d$  transitions noted at  $20\,700$  and  $29\,400\text{ cm}^{-1}$ . An analysis of these data similar to that described above for  $\text{CrF}_4$  gives  $Dq = 2\,125 \pm 100\text{ cm}^{-1}$ , with  $B' = 580 \pm 100\text{ cm}^{-1}$ , and  $\beta = 0.56$ .

**E.S.R. Studies.**—Intense e.s.r. signals were observed from powdered samples of  $\text{CrF}_5$  and  $\text{CsCrF}_6$ . At  $-196^\circ\text{C}$ ,  $\text{CrF}_5$  gave a broad, asymmetric, structureless feature centred at  $g$  ca. 2.0, whilst  $\text{CsCrF}_6$  gave a single line at  $g = 1.93$ .

**Matrix Isolation I.R. Studies.**—Matrix isolation studies on  $\text{CrF}_4$ ,  $\text{CrF}_5$ , and  $\text{CrF}_6$  were carried out in an attempt to characterise their products of vaporisation. The only previous reports\* on vapour species from these systems were a series of mass-spectrometric/electric deflection observations<sup>6,12,13</sup> and the publication by Glemser and co-workers<sup>10</sup> of a (complex) i.r. spectrum obtained by condensing  $\text{CrF}_6$  vapour onto a CsBr

\* Note added in proof: An electron diffraction study has recently been reported (E. J. Jacob, L. Hedberg, K. Hedberg, H. Davis, and G. L. Gard, *J. Phys. Chem.*, 1984, **88**, 1935) on the vapour species produced by heating  $\text{CrF}_5$  to ca.  $80^\circ\text{C}$ . The scattering curve is interpreted in terms of monomeric  $\text{CrF}_5$  with  $C_{2v}$  symmetry.

**Table 1.** Selected spectroscopic data for fluorides of Cr, Mo, and W

	CrF <sub>4</sub>		CrF <sub>5</sub>		Cs <sub>2</sub> CrF <sub>6</sub> solid
	solid	Ar matrix	solid	liquid <sup>a</sup>	
Principal i.r. bands (cm <sup>-1</sup> )	{ 830—750 550—490 ca. 290	{ 784.3 — 303	{ 830—750 600—450 ca. 300	{ 820—650 580—400 ca. 250	ca. 580
Stretching constant <sup>b</sup>		4.76			
Principal u.v.-visible bands (cm <sup>-1</sup> )	{ 35 000—40 000 28 000 21 000 13 500 12 350	{ 32 700 22 000 (sh)	{ 37 000 26 000 22 400		{ 30 000—40 000 29 400 20 700
Principal i.r. bands (cm <sup>-1</sup> )	{ CsCrF <sub>6</sub> solid ca. 600	{ CrF <sub>6</sub> N <sub>2</sub> matrix 758.9	{ MoF <sub>6</sub> gas <sup>c</sup> 741 — 262	{ WF <sub>6</sub> gas <sup>c</sup> 711 — 258	
Stretching constant <sup>c</sup>		3.86—3.92	4.38	4.71	
Principal u.v.-visible bands (cm <sup>-1</sup> )	{ 30 000—43 000 24 150 21 100 (sh)	{ 38 450 31 250 26 700	{ 57 500 52 750 47 600	{ 69 350 63 100—66 700 58 350	

<sup>a</sup> From ref. 11. <sup>b</sup> The value tabulated is for the diagonal *F*-matrix element (mdyn Å<sup>-1</sup>) for the i.r.-active stretching mode. <sup>c</sup> From refs. 26 and 31.

**Table 2.** Observed<sup>a</sup> and calculated vibration frequencies (cm<sup>-1</sup>) for matrix-isolated CrF<sub>4</sub> and CrF<sub>6</sub>

(i) CrF <sub>4</sub>	Observed	Calculated <sup>b</sup>	Assignment <sup>c</sup>	Observed	Assignment <sup>d</sup>	
	(Ar)					(N <sub>2</sub> )
	789.5	789.4	<sup>50</sup> Cr	796.0	$\left. \begin{array}{l} \sup{50}\text{Cr} \\ \sup{52}\text{Cr} \\ \sup{53}\text{Cr} \\ \sup{54}\text{Cr} \end{array} \right\} B_2(?)$ $\left. \begin{array}{l} \sup{50}\text{Cr} \\ \sup{52}\text{Cr} \\ \sup{53}\text{Cr} \\ \sup{54}\text{Cr} \end{array} \right\} E(?)$	
	788.2	—	S	790.6		
	786.6	—	S	788.0		
	784.3	784.3	<sup>52</sup> Cr	785.7		
	783.0	—	S	780.7		
	781.8	781.9	<sup>53</sup> Cr	778.5		
	780.5	—	S	776.4		
	779.5	779.5	<sup>54</sup> Cr			
	778.3	—	S			
	303	303	(T <sub>2</sub> bend)	304		('T <sub>2</sub> ' bend)
(ii) CrF <sub>6</sub>	Observed	Assignment	Observed	Calculated <sup>e</sup>		Assignment
	(Ar)			(N <sub>2</sub> )	I	
	769.6	<sup>50</sup> Cr	765.3	765.3	765.3	$\left. \begin{array}{l} \sup{50}\text{Cr} \\ \sup{52}\text{Cr} \\ \sup{53}\text{Cr} \\ \sup{54}\text{Cr} \end{array} \right\} T_{1u}$ (T <sub>1u</sub> )
	763.2	<sup>52</sup> Cr	758.9	758.9	758.9	
	760.0	<sup>53</sup> Cr	755.8	755.9	755.9	
	757.1	<sup>54</sup> Cr	753.0	752.9	753.0	
	—	—	—	250	300	

<sup>a</sup> Frequency accuracy ±0.3 cm<sup>-1</sup>. <sup>b</sup> Assuming force constants *F*<sub>33</sub>, *F*<sub>34</sub>, and *F*<sub>44</sub> of 4.76, 0.20, and 0.31 mdyn Å<sup>-1</sup>. <sup>c</sup> Bands denoted S are assigned to CrF<sub>4</sub> molecules trapped on minor sites. <sup>d</sup> Assuming a distortion to D<sub>2d</sub> symmetry. <sup>e</sup> Assuming force constants *f*<sub>33</sub>, *f*<sub>34</sub>, and *f*<sub>44</sub>: I, 3.86, 0.16, and 0.19; II, 3.92, 0.23, and 0.27 mdyn Å<sup>-1</sup>.

window cooled to -180 °C. As a result of preliminary studies on these binary systems, we also became interested in the vaporisation of the salt CsCrF<sub>6</sub>. Both CrF<sub>4</sub> and CrF<sub>5</sub> are polymeric in their condensed phases, whilst CsCrF<sub>6</sub> almost certainly contains discrete [CrF<sub>6</sub>]<sup>-</sup> units. Its thermal decomposition might therefore provide a simple route to monomeric CrF<sub>5</sub>.

The matrix i.r. spectra obtained from these systems all showed intense absorptions in the Cr-F stretching region (600—850 cm<sup>-1</sup>) and the region down to 200 cm<sup>-1</sup> was also routinely scanned in a search for bending modes. In view of the reactivity

of these systems towards hydrolysis, the spectral region 1 100—1 000 cm<sup>-1</sup> was also examined in detail for evidence of ν<sub>Cr=O</sub> bands. Both CrOF<sub>4</sub> and CrO<sub>2</sub>F<sub>2</sub> are potential contaminants, and would be volatile at the temperatures employed in these vaporisations.

Another general feature of these spectra was the occurrence of weak satellite peaks accompanying the most intense absorptions. These arise from the natural distribution of chromium isotopes (<sup>50</sup>Cr, 4.5%; <sup>52</sup>Cr, 83.8%; <sup>53</sup>Cr, 9.4%; <sup>54</sup>Cr, 2.3%) and in addition to revealing vibrational motion involving one atom of chromium, this pattern may also be used quantitatively

as a preliminary indication of structure. The isotope shifts associated with i.r.-active Cr-F stretching modes are, in general, angle dependent. Thus for the antisymmetric stretch of a linear F-Cr-F unit, such as would be found in octahedral  $\text{CrF}_6$  or square-planar  $\text{CrF}_4$ , an overall  $^{50}\text{Cr}$ - $^{54}\text{Cr}$  separation of *ca.*  $12.4\text{ cm}^{-1}$  at  $760\text{ cm}^{-1}$  can be estimated, whilst for tetrahedral  $\text{CrF}_4$ , this separation will be only *ca.*  $9.6\text{ cm}^{-1}$ .

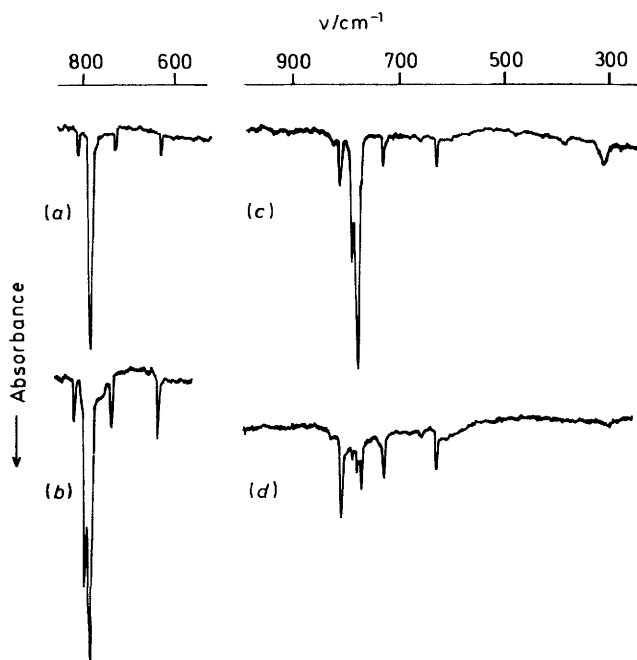


Figure 1. I.r. matrix spectra obtained from (a)  $\text{CrF}_4$  (Ar), (b)  $\text{CrF}_4$  ( $\text{N}_2$ ), and (c)  $\text{CsCrF}_6$  ( $\text{N}_2$ ) before diffusion; (d) as (c), after diffusion

A considerable number of experiments were carried out on these systems employing argon and nitrogen as matrix gases, and the vaporisation of  $\text{CrF}_5$  was also studied in a krypton matrix. However, only seven of these need to be discussed in any detail, and the numerical results from these experiments are summarised in Tables 1 and 2.

$\text{CrF}_4$  and  $\text{CsCrF}_6$ . When samples of  $\text{CrF}_4$  were heated to *ca.*  $110$ – $120^\circ\text{C}$ , and the vapours condensed in an argon matrix, the i.r. spectrum was typically found to contain an intense absorption centred at  $784.3\text{ cm}^{-1}$  together with weaker features at  $810$ ,  $730$ ,  $632$ , and  $303\text{ cm}^{-1}$ . Variations in deposition conditions indicated that the bands at  $784.3$  and  $303\text{ cm}^{-1}$  were due to a single species which predominated in more dilute matrices, whilst the remaining three features were more prominent in concentrated matrices. Figure 1(a) shows a typical spectrum obtained in the Cr-F stretching region. In nitrogen matrices, a similar pattern of weaker bands was observed ( $812$ ,  $730$ ,  $629$ , and  $304\text{ cm}^{-1}$ ), but the most intense feature now appeared as a doublet with components at  $790.6$  and  $780.7\text{ cm}^{-1}$  [Figure 1(b)].

Figure 1(c) shows the nitrogen matrix spectrum obtained from the vaporisation of  $\text{CsCrF}_6$  at *ca.*  $220^\circ\text{C}$ . This spectrum is essentially identical to that obtained from  $\text{CrF}_4$ , and controlled diffusion studies confirmed the isolation of two different species. When the deposit shown in Figure 1(c) was warmed to *ca.*  $25\text{ K}$ , there was a rapid decrease in the intensity of the  $790.6/780.7\text{ cm}^{-1}$  doublet, and of the lower frequency feature at  $304\text{ cm}^{-1}$ , but the features at  $812$ ,  $730$ , and  $629\text{ cm}^{-1}$  all increased in intensity. At the same time, a new band at  $772\text{ cm}^{-1}$  emerged from the shoulder of the lower frequency component of the doublet. Figure 1(d) shows the extent of these spectral changes.

It would therefore appear that  $\text{CrF}_4$  and  $\text{CsCrF}_6$  yield essentially the same matrix isolation i.r. spectra, and that behaviour characteristic of a monomer  $\rightarrow$  polymer reaction occurs on diffusion. We therefore provisionally assign the intense doublet observed in nitrogen matrices ( $790.6/780.7\text{ cm}^{-1}$ )

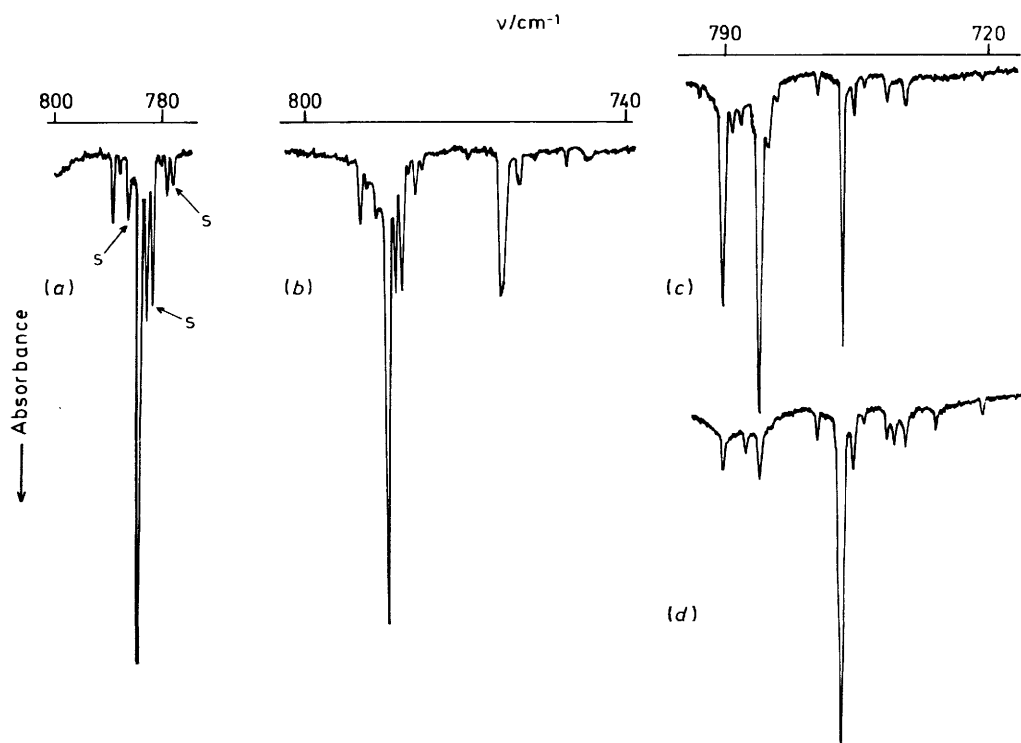


Figure 2. Higher resolution i.r. spectra of principal features obtained from (a)  $\text{CrF}_4$  (Ar), (b)  $\text{CrF}_5$  (Ar), (c)  $\text{CrF}_5$  ( $\text{N}_2$ ), (d)  $\text{CrF}_6$  ( $\text{N}_2$ )

and its accompanying band at  $304\text{ cm}^{-1}$  to monomeric  $\text{CrF}_4$ , and propose the same assignment for the corresponding argon matrix features at  $784.3$  and  $303\text{ cm}^{-1}$ .

Figure 2(a) shows the argon matrix band at  $784.3\text{ cm}^{-1}$  under higher resolution. At least seven sharp components may be distinguished, and this pattern is clearly more complex than would be expected for the natural distribution of  $\text{CrF}_4$  isotopomers. However, it is evident that the most intense component at  $784.3\text{ cm}^{-1}$  must correspond to a species containing  $^{52}\text{Cr}$  (83.8% abundant), and on the basis of their intensities and relative spacings from this band, the weaker peaks at  $789.5$ ,  $781.8$ , and  $779.5\text{ cm}^{-1}$  are assigned to the isotopomers  $^{50}\text{CrF}_4$ ,  $^{53}\text{CrF}_4$ , and  $^{54}\text{CrF}_4$ . The magnitude of the  $^{50}\text{Cr}$ - $^{54}\text{Cr}$  separation ( $10.0\text{ cm}^{-1}$ ) indicates a tetrahedral rather than a square-planar structure. The additional bands at  $788.2$ ,  $786.6$ ,  $783.0$ ,  $780.5$ , and  $778.3\text{ cm}^{-1}$  (denoted S) are attributed to  $\text{CrF}_4$  molecules trapped on other sites.

Tetrahedral  $\text{CrF}_4$  would be expected to have a  $^3A_2$  ground state, and should not show any static Jahn-Teller distortion. For a  $T_d$   $\text{MX}_4$  species,  $\Gamma_{\text{vib}} = A_1 + E + 2T_2$ . The absorptions at  $784.3$  and  $303\text{ cm}^{-1}$  are thus assigned as the  $T_2$  stretch and  $T_2$  bend respectively, and this assignment is supported by an analysis of the isotope pattern for the stretch.

The secular equations for these  $T_2$  modes are summarised in the Appendix, and it is evident that three independent force-constant parameters are required for their solution. Using the  $^{52}\text{CrF}_4$  argon matrix absorptions at  $784.3$  and  $303\text{ cm}^{-1}$ , it is found that the observed isotope pattern is reproduced to within experimental error by taking values of 4.76, 0.31, and  $0.20\text{ mdyne \AA}^{-1}$  for  $F_{33}$ ,  $F_{44}$ , and  $F_{34}$  respectively (Table 2).

In nitrogen matrices, the most intense feature from  $\text{CrF}_4$  vapourisation is a doublet at  $790.6/780.7\text{ cm}^{-1}$ . This doublet could arise from ( $T_d$ )  $\text{CrF}_4$  trapped on two different sites, but estimates of the intensity ratio of these bands suggest an alternative explanation. Experimentally, it is found that these bands have a constant intensity ratio very close to 1:2, and this could arise from a splitting of the  $T_2$  degeneracy into, for example,  $A_1 + E$  in  $C_{3v}$  symmetry, or  $B_2 + E$  in  $D_{2d}$ . A similar lifting of degeneracy has been noted for other species isolated in nitrogen matrices.<sup>16,20</sup> In principle, these two possible explanations for the doublet may be distinguished by a consideration of the isotope structure on each component. Although these isotope patterns overlap in the region  $780$ – $790\text{ cm}^{-1}$  [Figure 2(b)] the  $^{50}\text{Cr}$ - $^{52}\text{Cr}$  shift for the higher frequency component, and the  $^{52}\text{Cr}$ - $^{54}\text{Cr}$  shift for the lower frequency component can be measured to within  $\pm 0.2\text{ cm}^{-1}$ .

As indicated earlier, these shifts are angle dependent, but for  $T_d$  isotopomers trapped in similar sites, they should be almost identical. In argon matrices, where one site predominates, values of  $5.2$  and  $4.8\text{ cm}^{-1}$  (both  $\pm 0.2\text{ cm}^{-1}$ ) are obtained for the  $^{50}\text{Cr}$ - $^{52}\text{Cr}$  and  $^{52}\text{Cr}$ - $^{54}\text{Cr}$  shifts respectively. In nitrogen matrices, the  $^{50}\text{Cr}$ - $^{52}\text{Cr}$  shift for the higher frequency component is  $5.4\text{ cm}^{-1}$ , whilst the  $^{52}\text{Cr}$ - $^{54}\text{Cr}$  shift for the more intense lower frequency component is only  $4.6\text{ cm}^{-1}$ . This difference is outside experimental error, and thus indicates an angle distortion from  $T_d$  symmetry and hence a lifting of the  $T_2$  degeneracy. In particular, a simple analysis analogous to that described for molecular  $\text{K}_2\text{CrO}_4$ <sup>25</sup> shows that both the ca. 1:2 intensity ratio and the differing isotope shifts are consistent with a distortion to  $D_{2d}$  symmetry in which the  $B_2$  and  $E$  components lie at  $790.6$  and  $780.7\text{ cm}^{-1}$  respectively.

$\text{CrF}_5$  and  $\text{CrF}_6$ . Samples of  $\text{CrF}_5$  yielded vapour species at considerably lower temperatures than were necessary for  $\text{CrF}_4$ , and Figure 2(b) shows part of an argon matrix spectrum obtained from a  $\text{CrF}_5$  sample at ca.  $55^\circ\text{C}$ . It is evident that the most prominent band centred at  $784.3\text{ cm}^{-1}$  is very similar to the multiplet previously assigned to  $\text{CrF}_4$ , the only significant differences being the lower relative intensities of those

absorptions (denoted S) attributed to  $^{52}\text{CrF}_4$  molecules trapped on minor sites. However in addition to these  $\text{CrF}_4$  absorptions, this spectrum also shows a prominent new band at  $763.2\text{ cm}^{-1}$ .

A typical nitrogen matrix spectrum obtained from  $\text{CrF}_5$  is shown in Figure 2(c). The two intense bands at  $790.6$  and  $780.7\text{ cm}^{-1}$  are due to  $\text{CrF}_4$ , and the spectrum also exhibits an intense absorption at  $758.9\text{ cm}^{-1}$ . This clearly shows the characteristic chromium isotope pattern, and corresponds to the argon matrix absorption at  $763.2\text{ cm}^{-1}$  in Figure 2(b). The weak bands at ca.  $746.6$  and  $741.8\text{ cm}^{-1}$  are due to  $\text{CrOF}_4$ <sup>16</sup> and this deposit also showed weak features at  $1027.7\text{ cm}^{-1}$  ( $\text{CrOF}_4$ ) and at  $304\text{ cm}^{-1}$  ( $\text{CrF}_4$ ).

Figure 2(d) shows the same spectral region after codeposition of a  $\text{CrF}_6$ - $\text{N}_2$  mixture with an excess of nitrogen. The band at  $758.9\text{ cm}^{-1}$  is now the most prominent feature, and this spectrum shows traces of  $\text{CrO}_2\text{F}_2$ ,  $\text{CrOF}_4$ , and  $\text{CrF}_4$  together with new weak bands at ca.  $745$  and  $734\text{ cm}^{-1}$ . However, despite a careful search in the low-frequency region, there was no obvious bending mode which could be associated with the intense absorption at  $758.9\text{ cm}^{-1}$ . In argon matrices, the spectrum obtained from  $\text{CrF}_6$ -Ar mixtures was qualitatively similar to that from  $\text{CrF}_5$  [Figure 2(b)] but the band at  $763.2\text{ cm}^{-1}$  was relatively more intense.

Finally, one experiment was carried out in which  $\text{CrF}_5$  was vapourised and co-condensed in a krypton matrix. Spectral quality was poorer than in argon or nitrogen, but the principal ( $^{52}\text{Cr}$ ) absorptions of  $\text{CrF}_4$  and  $\text{CrOF}_4$  were found at  $786.2$  and  $747\text{ cm}^{-1}$  respectively, and a prominent doublet (intensity ratio 1:2) was noted at  $762/758.2\text{ cm}^{-1}$ .

The spectra obtained from  $\text{CrF}_5$  and  $\text{CrF}_6$  thus all show absorption due to  $\text{CrF}_4$ , but the most significant new feature is an intense absorption at ca.  $760\text{ cm}^{-1}$ . This band shows isotope structure consistent with the motion of one atom of chromium, and it is the only prominent feature observed from samples of  $\text{CrF}_6$  [Figure 2(d)]. The  $^{50}\text{Cr}$ - $^{54}\text{Cr}$  frequency shift of ca.  $12.4\text{ cm}^{-1}$  (Table 2) indicates a linear F-Cr-F unit, and it is therefore assigned as the  $T_{1u}$  stretching mode in octahedral  $\text{CrF}_6$ . The related species  $\text{MoF}_6$  and  $\text{WF}_6$  are known to possess  $O_h$  symmetry, and have  $T_{1u}$  stretching modes at  $741$  and  $711\text{ cm}^{-1}$  respectively.<sup>26</sup>

In addition to showing a single  $T_{1u}$  stretching mode, the i.r. spectrum of  $\text{CrF}_6$  should contain one  $T_{1u}$  bending mode. This bending mode is found at  $262\text{ cm}^{-1}$  in  $\text{MoF}_6$  and at  $258\text{ cm}^{-1}$  in  $\text{WF}_6$ , and we therefore expect the bend in  $\text{CrF}_6$  to lie in the frequency region  $250$ – $300\text{ cm}^{-1}$ . As was the case for  $\text{CrF}_4$ , the secular equations for the i.r.-active modes in  $\text{CrF}_6$  require three force-constant parameters for their solution (see Appendix). In the absence of an experimental value for the bend we therefore selected arbitrary values of  $250$ ,  $275$ , and  $300\text{ cm}^{-1}$  and calculated three sets of force constants which gave a satisfactory fit for the isotope structure on the stretching mode. Two of these sets are included in Table 2. In view of this additional assumption inherent in the  $\text{CrF}_6$  analysis, it would be unwise to treat these force constants too seriously, but it is significant that the stretching constant  $f_{33}$  is relatively insensitive to the uncertainty in the position of the bending mode. In addition, this parameter, which represents  $f_r - f_{rr}$  in a valence force field, is significantly lower than the analogous parameter in  $\text{MoF}_6$  and  $\text{WF}_6$  (see Table 1). This difference points to a relatively weak bond in  $\text{CrF}_6$  and is consistent with low thermal stability and high reactivity.

*Matrix Isolation Ultraviolet-Visible Studies on  $\text{CrF}_4$  and  $\text{CrF}_6$ .*—U.v.-visible spectra were obtained from samples of  $\text{CrF}_4$  and  $\text{CrF}_6$  using argon as a matrix gas, and employing deposition conditions similar to those described in the i.r. studies. Chromium tetrafluoride samples gave spectra which consisted of an intense c.t. band at ca.  $32\,700\text{ cm}^{-1}$  with a long

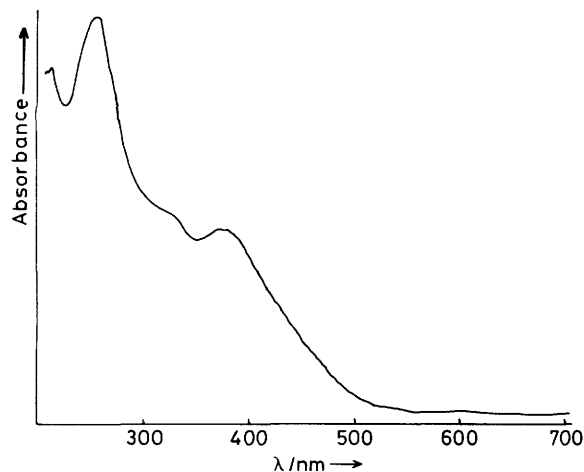


Figure 3. U.v.-visible spectrum of  $\text{CrF}_6$  isolated in an argon matrix

tail into the visible region. After extended deposition, a weak shoulder became apparent at *ca.*  $22\,000\text{ cm}^{-1}$ , but no additional well defined features were detected.

For a  $d^2$  ion in  $T_d$  symmetry, three spin-allowed  $d-d$  bands are expected. In order of increasing energy, these are  ${}^3A_2 \rightarrow {}^3T_2(F)$  ( $\nu_1$ ),  ${}^3A_2 \rightarrow {}^3T_1(F)$  ( $\nu_2$ ), and  ${}^3A_2 \rightarrow {}^3T_1(P)$  ( $\nu_3$ ). The lowest of these corresponds to  $10Dq$ , and using the value of  $22\,000\text{ cm}^{-1}$  for this parameter in solid ( $O_h$ )  $\text{CrF}_4$ , we estimate that  $\nu_1$  for molecular  $\text{CrF}_4$  will occur at *ca.*  $9\,500\text{ cm}^{-1}$  and thus lie below the limit of our spectrometer. It is possible that the shoulder at  $22\,000\text{ cm}^{-1}$  corresponds to  $\nu_3$  [*cf.*  $\nu_3$  in  $\text{Cr}(\text{OBU}^t)_4$  at  $25\,000\text{ cm}^{-1}$ ]<sup>27</sup> but if so, we would expect to see  $\nu_2$  at *ca.*  $13\,000\text{--}15\,000\text{ cm}^{-1}$ .

It would therefore seem likely that in comparison with the intense band at  $32\,700\text{ cm}^{-1}$ , the absorption coefficients of the  $d-d$  bands are very small, and that they are masked by the low-energy tail. We also note that some difficulty has been encountered in the assignment of the  $d-d$  spectra of tetrahedral  $\text{Cr}^{\text{IV}}$  compounds.<sup>28,29</sup>

The u.v.-visible spectrum of  $\text{CrF}_6$  in argon is shown in Figure 3. Sample deposition was conducted in a similar way to the i.r. studies, except that the spray-on tube was cooled to *ca.*  $-20^\circ\text{C}$  to minimise the formation of impurities during deposition. The spectrum consists of three main bands at *ca.*  $38\,450$ ,  $31\,250$ , and  $26\,700\text{ cm}^{-1}$ , with a long tail into the visible region. The transition at  $26\,700\text{ cm}^{-1}$  is of comparable energy to the lowest  $\text{F} \rightarrow \text{Cr}$  c.t. band in  $\text{CrOF}_4$  ( $27\,000\text{ cm}^{-1}$ )<sup>16</sup> and is consistent with the predictions of the optical electro-negativity model.<sup>23</sup>

A more detailed assignment may, however, be made by comparison with the spectra of  $\text{MoF}_6$  and  $\text{WF}_6$ .<sup>30,31</sup> For an  $O_h$   $\text{MF}_6$  molecule, the c.t. bands  $\pi(\text{F}) \rightarrow \text{Cr}(t_{2g})$  are, in order of increasing energy,<sup>31</sup>  $t_{1g} \rightarrow t_{2g}$ ,  $t_{1u} \rightarrow t_{2g}$ , and  $t_{2u} \rightarrow t_{2g}$ , and these provide a basis for assigning the three observed transitions. In  $\text{WF}_6$ , these transitions lie at *ca.*  $58\,350$ , *ca.*  $63\,100\text{--}66\,700$ , and *ca.*  $69\,350\text{ cm}^{-1}$  whilst in  $\text{MoF}_6$  they occur at *ca.*  $47\,600$ , *ca.*  $52\,750$ , and *ca.*  $57\,500\text{ cm}^{-1}$ .<sup>31</sup> A further bathochromic shift of *ca.*  $20\,000\text{ cm}^{-1}$  between Mo and Cr would therefore account for the observed  $\text{CrF}_6$  transitions. An alternative possibility is that some of the  $\text{CrF}_6$  transitions arise from  $\pi(\text{F}) \rightarrow \text{Cr}(e_g)$  charge transfer. However, it seems unlikely that the  $t_{2g}-e_g$  separation in  $\text{CrF}_6$  is less than *ca.*  $25\,000\text{ cm}^{-1}$ , as  $10Dq$  in solid  $\text{CrF}_5$  is *ca.*  $24\,000\text{ cm}^{-1}$ , and this set of c.t. bands is therefore expected at much higher energy ( $> \text{ca. } 50\,000\text{ cm}^{-1}$ ). We therefore assign the  $\text{CrF}_6$  c.t. bands as  $\pi(\text{F}) \rightarrow \text{Cr}(t_{2g})$  transitions (Table 1).

Several of the absorptions in the gas-phase spectra of  $\text{MoF}_6$  and  $\text{WF}_6$  show clearly resolved vibrational progressions which

have been correlated with  $A_{1g}(\text{M}-\text{F})$  stretches.<sup>31</sup> Our spectra of  $\text{CrF}_6$  in argon matrices showed little evidence of structure, but using second-derivative recording, a partially resolved progression of *ca.*  $530\text{ cm}^{-1}$  could be discerned on the lowest energy band (*ca.*  $26\,700\text{ cm}^{-1}$ ). The estimated value<sup>26</sup> for the  $A_{1g}$  stretch in the ground state is *ca.*  $720\text{ cm}^{-1}$ .

*Thermal Stability of  $\text{CrF}_6$  and  $\text{CrF}_5$ : Additional Observations.*—Although the principal vapour species obtained from samples of  $\text{CrF}_6$  appears to be molecular  $\text{CrF}_6$ , with some  $\text{CrF}_4$ ,  $\text{CrO}_2\text{F}_2$ , and  $\text{CrOF}_4$  impurity, prolonged deposition sometimes produced two weak bands at *ca.*  $734$  and *ca.*  $745\text{ cm}^{-1}$  [see Figure 2(d)] which did not correlate with any other known chromium fluoride species. The same bands were also occasionally observed after prolonged deposition from  $\text{CrF}_5$  samples, and although they were never sufficiently intense for a chromium isotope pattern to be observed, it is possible that they could be fundamentals of molecular  $\text{CrF}_5$ .

In their initial studies on the stability of  $\text{CrF}_6$ , Glemser and co-workers<sup>3,10</sup> noted that solid  $\text{CrF}_6$  readily decomposed into (solid)  $\text{CrF}_5 + \text{F}_2$ , and we also noted a colour change from yellow to red, consistent with this reaction, when solid samples of  $\text{CrF}_6$  were stored in the dry-box for short periods.

Although the matrix i.r. spectra obtained from samples of  $\text{CrF}_5$  appear to indicate complete disproportionation to  $\text{CrF}_4$  and  $\text{CrF}_6$ , it is possible that molecular  $\text{CrF}_5$  could be formed in the stepwise thermal decomposition of molecular  $\text{CrF}_6$ . In order to test this, a sequence of spectra was run in which the stainless-steel tube between the autoclave and the cryostat was slowly heated to *ca.*  $100^\circ\text{C}$  during a  $\text{CrF}_6$  deposition. Simultaneous monitoring of the i.r. spectrum over the region  $820\text{--}700\text{ cm}^{-1}$  clearly showed that as the temperature of the tube was raised the  $\text{CrF}_6$  band ceased to grow. However, this change was accompanied not by an increase in the bands at  $734$  and  $745\text{ cm}^{-1}$ , but the rapid growth of  $\text{CrF}_4$  monomer and polymer features.

We therefore conclude that the principal decomposition product of molecular  $\text{CrF}_6$  is  $\text{CrF}_4$ , and this would perhaps account for the complexity of Glemser's i.r. spectrum<sup>10</sup> of 'solid  $\text{CrF}_6$ '. The disproportionation of  $\text{CrF}_5$  at low pressures is similar to that found for  $\text{WF}_5$ ,<sup>32</sup> and could account for certain anomalies found in connection with the mass-spectrometric data obtained for  $\text{CrF}_5$ .

As indicated earlier, samples of  $\text{CrF}_5$  have been studied by mass spectrometry<sup>6</sup> and by molecular beam electric deflection.<sup>13</sup> At  $25^\circ\text{C}$ , the relative intensities of the ion currents due to  $[\text{CrF}_5]^+$ ,  $[\text{CrF}_4]^+$ ,  $[\text{CrF}_3]^+$ ,  $[\text{CrF}_2]^+$ ,  $[\text{CrF}]^+$ , and  $\text{Cr}^+$  were found to be 0.048, 1.00, 0.85, 0.25, 0.32, and 0.38 respectively, whilst at  $90^\circ\text{C}$  the relative intensities of the first four of these were 0.026, 0.52, 1.0, and 0.5.<sup>13</sup> No evidence for polymeric species was found from these studies, and in the absence of any other information, the authors regarded all these ions as arising essentially from molecular  $\text{CrF}_5$ . However, they noted that the relative abundances of these ions were unusual, and suggested that contamination by  $\text{CrF}_4$ , or possibly disproportionation, might account for this. Nevertheless, they regarded  $\text{CrF}_5$  as the only neutral precursor for  $[\text{CrF}_5]^+$  and concluded on the basis of a small refocussing effect,<sup>13</sup> that  $\text{CrF}_5$  did not have  $D_{3h}$  symmetry.

If our conclusions regarding the vaporisation of  $\text{CrF}_5$  are correct, it is evident that  $\text{CrF}_6$  is the most likely neutral precursor for  $[\text{CrF}_5]^+$ . Either disproportionation, or the thermal decomposition of  $\text{CrF}_6$  could then account for the anomalous proportions of  $[\text{CrF}_4]^+$  and  $[\text{CrF}_3]^+$  ions. The refocussing effect observed for  $[\text{CrF}_5]^+$  could arise from a vibrationally induced dipole in ( $O_h$ )  $\text{CrF}_6$ , and although early studies on other transition-metal hexafluorides have not shown this effect,<sup>33</sup> thermally accessible polar states have been invoked

to account for the refocussing behaviour observed for  $\text{CrF}_4$  and  $\text{TiF}_4$ .<sup>13</sup>

### Appendix

Vibrational analyses for  $\text{CrF}_4$  ( $T_d$ ) and  $\text{CrF}_6$  ( $O_h$ ) were based on secular equations derived using the Wilson matrix method.<sup>34</sup>

For  $\text{CrF}_4$ , suitable symmetry co-ordinates for the  $T_2$  modes are:  $S_3 = \frac{1}{2}(R_1 + R_2 - R_3 - R_4)$  and  $S_4 = \frac{R}{\sqrt{2}}(\theta_{12} - \theta_{34})$

where  $R_1$  is the Cr-F(1) bond, and  $\theta_{12}$  is the F(1)-Cr-F(2) angle. The corresponding  $G$ -matrix elements are then:  $G_{33} = \frac{1}{M_F} + \frac{4}{3M_{Cr}}$ ,  $G_{44} = \frac{2}{M_F} + \frac{16}{3M_{Cr}}$ , with  $G_{34} = G_{43} = -\frac{8}{3M_{Cr}}$ . The  $F$ -matrix elements  $F_{33}$ ,  $F_{44}$  and  $F_{34}$  ( $= F_{43}$ ) were evaluated directly.

In the case of  $\text{CrF}_6$ , with F(1) and F(2) *trans* the symmetry co-ordinates  $s_3 = \frac{1}{\sqrt{2}}(r_1 - r_2)$  and  $s_4 = \frac{r}{2\sqrt{2}}(\theta_{13} + \theta_{14} + \theta_{15} + \theta_{16} - \theta_{23} - \theta_{24} - \theta_{25} - \theta_{26})$  for the  $T_{1u}$  modes lead to the elements  $g_{33} = \frac{1}{M_F} + \frac{2}{M_{Cr}}$ ,  $g_{44} = \frac{2}{M_F} + \frac{8}{M_{Cr}}$ , and  $g_{34} = g_{43} = -\frac{4}{M_{Cr}}$ .

The force constants  $f_{33}$ ,  $f_{44}$ , and  $f_{34}$  were again evaluated directly, and it is worth noting, for comparative purposes, that  $f_{33} = f_r - f_{rr}$  and  $F_{33} = F_R - F_{RR}$ .

The vibrational analysis of  $\text{XY}_6$  ( $O_h$ ) species has a chequered history<sup>35-38</sup> but these expressions are identical to those obtained by Claassen,<sup>39</sup> and are believed to be correct.

### Acknowledgements

We gratefully acknowledge the financial support of the S.E.R.C. for this work, and wish to thank Professor I. R. Beattie for helpful discussions.

### References

- 1 For a review, see R. Colton and J. H. Canterford, 'Halides of the First Row Transition Elements,' Wiley, New York, 1968.
- 2 H. von Wartenberg, *Z. Anorg. Allg. Chem.*, 1941, **247**, 135.
- 3 O. Glemser, H. Roesky, and K. H. Hellberg, *Angew. Chem., Int. Ed. Engl.*, 1963, **2**, 266.
- 4 A. J. Edwards, *Proc. Chem. Soc.*, 1963, 205.
- 5 T. A. O'Donnell and D. F. Stewart, *Inorg. Chem.*, 1966, **5**, 1434.
- 6 A. J. Edwards, W. E. Falconer, and W. A. Sunder, *J. Chem. Soc., Dalton Trans.*, 1974, 541.
- 7 J. Slivnik and B. Zemva, *Z. Anorg. Allg. Chem.*, 1971, **385**, 137.

- 8 S. D. Brown, T. M. Loehr, and G. L. Gard, *J. Fluorine Chem.*, 1976, **7**, 19.
- 9 H. C. Clark and Y. N. Sadana, *Can. J. Chem.*, 1964, **42**, 50.
- 10 K. H. Hellberg, A. Muller, and O. Glemser *Z. Naturforsch., Teil B*, 1966, **21**, 118.
- 11 S. D. Brown, T. M. Loehr, and G. L. Gard, *J. Chem. Phys.*, 1976, **64**, 260.
- 12 M. J. Vasile, G. R. Jones, and W. E. Falconer, *Int. J. Mass. Spectrosc.*, 1972, **10**, 457.
- 13 W. E. Falconer, G. R. Jones, W. A. Sunder, M. J. Vasile, A. A. Muentner, T. R. Dyke, and W. Klemperer, *J. Fluorine Chem.*, 1974, **4**, 213.
- 14 W. Levason, J. S. Ogden, and A. J. Rest, *J. Chem. Soc., Dalton Trans.*, 1980, 419.
- 15 E. G. Hope, P. J. Jones, W. Levason, J. S. Ogden, M. Tajik, and J. W. Turff, *J. Chem. Soc., Dalton Trans.*, 1984, 2445.
- 16 E. G. Hope, P. J. Jones, W. Levason, J. S. Ogden, M. Tajik, and J. W. Turff, *J. Chem. Soc., Dalton Trans.*, 1985, 529.
- 17 I. R. Beattie, C. J. Marsden, and J. S. Ogden, *J. Chem. Soc., Dalton Trans.*, 1980, 535.
- 18 E. G. Hope, P. J. Jones, W. Levason, J. S. Ogden, and M. Tajik, *J. Chem. Soc., Chem. Commun.*, 1984, 1355.
- 19 R. Hoppe, *Angew. Chem., Int. Ed. Engl.*, 1981, **20**, 63.
- 20 W. Levason, R. Narayanaswamy, J. S. Ogden, A. J. Rest, and J. W. Turff, *J. Chem. Soc., Dalton Trans.*, 1981, 2501.
- 21 See, for example, A. F. Wells, 'Structural Inorganic Chemistry,' 4th edn., Oxford University Press, 1975, p. 326.
- 22 See, for example, A. B. P. Lever, 'Inorganic Electronic Spectroscopy,' Elsevier, Amsterdam, 1968.
- 23 C. K. Jorgensen, *Prog. Inorg. Chem.*, 1970, **12**, 101.
- 24 H. Bode and E. Voss, *Z. Anorg. Allg. Chem.*, 1956, **286**, 136; G. C. Allen and G. A. M. el-Sharkawy, *Inorg. Nucl. Chem. Lett.*, 1970, **6**, 493.
- 25 I. R. Beattie, J. S. Ogden, and D. D. Price, *J. Chem. Soc., Dalton Trans.*, 1982, 505.
- 26 B. Weinstock and G. L. Goodman, *Adv. Chem. Phys.*, 1965, **9**, 169.
- 27 E. C. Alyea, J. S. Basi, D. C. Bradley, and M. H. Chisholm, *J. Chem. Soc. A*, 1971, 772.
- 28 W. Mowat, A. Shortland, G. Yagupsky, N. J. Hill, M. Yagupsky, and G. Wilkinson, *J. Chem. Soc., Dalton Trans.*, 1972, 533.
- 29 J. S. Basi, D. C. Bradley, and M. H. Chisholm, *J. Chem. Soc. A*, 1971, 1433.
- 30 K. N. Tanner and A. B. F. Duncan, *J. Am. Chem. Soc.*, 1951, **73**, 1164.
- 31 R. McDiarmid, *J. Chem. Phys.*, 1974, **61**, 3333.
- 32 J. Schroder and F. J. Grewe, *Chem. Ber.*, 1970, **103**, 1536.
- 33 E. W. Kaiser, J. S. Muentner, W. Klemperer, W. E. Falconer, and W. A. Sunder, *J. Chem. Phys.*, 1970, **53**, 1411.
- 34 See, for example, E. B. Wilson, J. C. Decius, and P. C. Cross, 'Molecular Vibrations,' McGraw-Hill, New York, 1955.
- 35 N. S. S. Nath, *Proc. Indian Acad. Sci.*, 1934, **1**, 250.
- 36 A. D. Liehr and C. J. Ballhausen, *Ann. Phys. NY*, 1958, **3**, 304.
- 37 D. F. Heath and J. W. Linnett, *Trans. Faraday Soc.*, 1949, **45**, 264.
- 38 K. Venkateswarlu and S. Sundaram, *Z. Phys. Chem.*, 1956, **9**, 174.
- 39 H. H. Claassen, *J. Chem. Phys.*, 1959, **30**, 968.

Received 10th September 1984; Paper 4/1565